Acta Crystallographica Section B
Structural Science
ISSN 0108-7681

Two new silicate structures based on a rhodesite-type heteropolyhedral microporous framework

Marcella Cadoni[a,b] and Giovanni Ferraris[a,b]*

[a]Dipartimento di Scienze Mineralogiche e Petrologiche, Università di Torino, Via Valperga Caluso 35, I-10125, Torino, Italy, and [b]Nanostructured Interfaces and Surfaces (NIS) Centre of Excellence, Via Pietro Giuria 7, I-10125 Torino, Italy

Correspondence e-mail: giovanni.ferraris@unito.it

Received 9 October 2009
Accepted 20 November 2009

Two new members of the mero-plesiotype rhodesite series [$Sr_2Na_2(Si_8O_{19})\cdot 4H_2O$, abbreviated as TR09; $SrNa_4(Si_8O_{19})\cdot 4H_2O$, TR10] have been hydrothermally synthesized in Teflon-lined autoclaves at 503 K and structurally characterized using X-ray diffraction single-crystal data. The crystal structures were solved by direct methods and refined to R = 0.021 [TR09; 3317 reflections with $I_o > 2\sigma(I_o)$] and R = 0.033 [TR10; 5007 reflections with $I_o > 2\sigma(I_o)$]. Both structures are based on a rhodesite-type microporous heteropolyhedral framework, where two types of channels are within the double silicate layer that alternates with an 'octahedral' *O* sheet. The large Sr^{2+} cation constrains to the roughly ellipsoidal shape of the channels. The H_2O molecules are located both in the *O* sheets and in the channels, where they are loosely hydrogen bonded. The crystal-chemical features that allow flexibility to the rhodesite-type microporous heteropolyhedral framework and make it interesting for possible technological applications are discussed.

1. Introduction

For the purpose of finding new microporous crystalline materials for technological applications, heteropolyhedral frameworks offer a range of crystal-chemical opportunities far wider than do tetrahedral frameworks like zeolites (Rocha & Lin, 2005). In fact, the higher coordination polyhedra (*e.g.* octahedra) that occur in the heteropolyhedral frameworks can host a variety of cations. Heteropolyhedral microporous structures are well represented in the mineral realm (Ferraris & Merlino, 2005) and often were the incentive for the synthesis of new compounds suitable for technological applications (*e.g.* ion exchange and luminescence related to the presence of lanthanides in the framework).

Minerals and synthetic phases (Table 1) belonging to the rhodesite ($KCa_2[Si_8O_{18}(OH)]\cdot 6H_2O$; a = 23.416, b = 6.555, c = 7.050 Å, *Pmam*; Hesse *et al.*, 1992) mero-plesiotype series are modular microporous hydrous silicates based on a heteropolyhedral framework (Ferraris & Gula, 2005; Ferraris *et al.*, 2008). Their structures (Fig. 1; all figures of structures by *ATOMS*; Dowty, 2002) contain a double silicate layer that is formed *via* corner sharing of two apophyllite-like tetrahedral sheets and alternates with different types of 'octahedral' sheets (*O* sheet; Fig. 2); Na, K, Ca, Ba, Sr and lanthanides are typical 'octahedral' cations. Using the symbol M^mN^n to indicate the topology of a tetrahedral sheet built on *M* and *N* rings according to an *m*/*n* ratio (Krivovichev, 2009), the apophyllite-like sheet has the topology 4^18^1 based on four- and eight-rings only. The double silicate layer contains eight-membered channels along two different directions: either perpendicular or parallel to the rows of edge-sharing octahedra in the *O*

Table 1
Members of the rhodesite mero-plesiotype series.

Name	Chemical formula	a, b, c (Å), β (°)	Space group
Seidite-(Ce)[a]	$Na_4(Ce,Sr)_2\{Ti(OH)_2[Si_8O_{18}]\}(O,OH,F)_4\cdot 5H_2O$	24.61, 7.23, 14.53, 94.6	$C2/c$
Rhodesite[b]	$KCa_2[Si_8O_{18}(OH)]\cdot 6H_2O$	23.416, 6.555, 7.050	$Pmam$
Macdonaldite[c]	$BaCa_4[Si_8O_{18}(OH)]_2\cdot 10H_2O$	14.081, 13.109, 23.560	$Cmcm$
Delhayelite[d]	$K_4Na_2Ca_2[AlSi_7O_{19}]_2F_2Cl$	24.579, 7.057, 6.581	$Pmmn$
Hydrodelhayelite[e]†	$KCa_2[AlSi_7O_{17}(OH)_2]\cdot 3H_2O$	6.648, 23.846, 7.073	$Pn2_1m$
Monteregianite-(Y)[f]	$KNa_2Y[Si_8O_{19}]\cdot 5H_2O$	9.512, 23.956, 9.617, 93.85	$P2_1/n$
Fivegite[g]	$K_4Ca_2[AlSi_7O_{17}(O_{2-x}OH_x)][(H_2O)_{2-x}OH_x]Cl$	24.345, 7.037, 6.540	$Pm2_1n$
AV-5[h]	$KNa_2Ce[Si_8O_{19}]\cdot 5H_2O$	9.579, 24.053, 9.695, 93.654	$P2_1/n$
Eu-AV-9[i]	$KNa_2Eu[Si_8O_{19}]\cdot 5H_2O$	23.973, 14.040, 6.566, 90.35	$C2/m$
Tb-AV-9[i]	$KNa_2Tb[Si_8O_{19}]\cdot 5H_2O$	23.945, 14.019, 6.554, 90.288	$C2/m$
Er-AV-9[j]	$KNa_2Er[Si_8O_{19}]\cdot 5H_2O$	23.951, 14.013, 6.550, 90.288	$C2/m$
Nd-AV-9[k]	$KNa_2Nd[Si_8O_{19}]\cdot 5H_2O$	–	–
Gd-AV-9[k]	$KNa_2Nd[Si_8O_{19}]\cdot 5H_2O$	–	–
TR03[l]	$KNaCa_2[Si_8O_{19}]\cdot 5H_2O$	6.585, 23.776, 7.025	$Pn2_1m$
TR04[l]	$KNa_3Sr[Si_8O_{19}]\cdot 4.3H_2O$	6.5699, 23.7225, 7.0225, 91.81	$P2_1/m$
TR09[m]	$Sr_2Na[Si_8O_{19}]\cdot 4H_2O$	22.7681, 6.9352, 13.5789, 92.58	$C2/c$
TR10[m]	$SrNa_4[Si_8O_{19}]\cdot 4H_2O$	22.4102, 7.0292, 13.3140, 92.54	$P2/c$

(*a*) Ferraris *et al.* (2003); (*b*) Hesse *et al.* (1992); (*c*) Cannillo *et al.* (1968); (*d*) Pekov *et al.* (2009); (*e*) Ragimov *et al.* (1980); (*f*) Ghose *et al.* (1987); (*g*) Pekov *et al.* (2010); (*h*) Rocha *et al.* (2000); (*i*) Ananias *et al.* (2001); (*j*) Ananias *et al.* (2004); (*k*) Rocha *et al.* (2004) without crystal data; (*l*) Cadoni & Ferraris (2009); (*m*) this work. † The space group $Pn2_1m$ is consistent with the orientation of the cell adopted in the structure determination by Ragimov *et al.* (1980) and reported in this table. Dorfman & Chiragov (1979) [abstracted in *Am. Mineral.* **72**, 1024 (1987)] give erroneously $Pnm2_1$, as used by Chiragov & Dorfman (1981) with a cell where b and c are exchanged. The error on the space group has been propagated in several databases and handbooks of mineralogy.

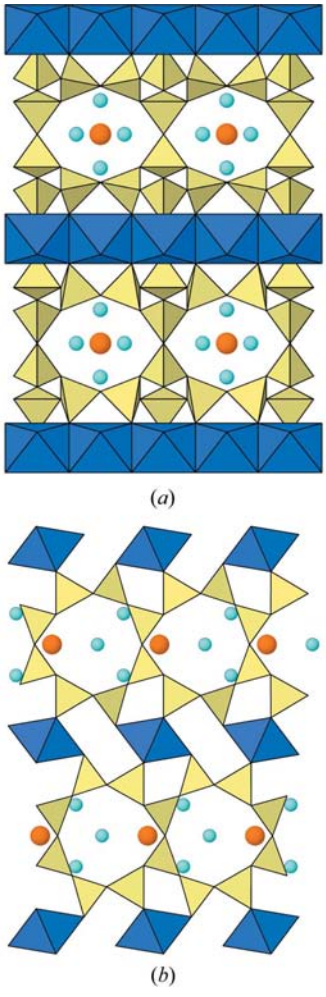

Figure 1
Crystal structure of rhodesite seen along (*a*) [010] and (*b*) [001]. Large and small circles represent K cations and H_2O molecules.

sheet. In rhodesite (Fig. 1) the first type of channel develops along [001] with an effective channel width (e.c.w.; McCusker *et al.*, 2003) in the range 3.5–3.8 Å; the second type is instead along [010] and its elliptical cross-section has an e.c.w. of *ca* 2.7 × 4.3 Å. With reference to the direction of the octahedral rows, the same situation is observed in other members of the

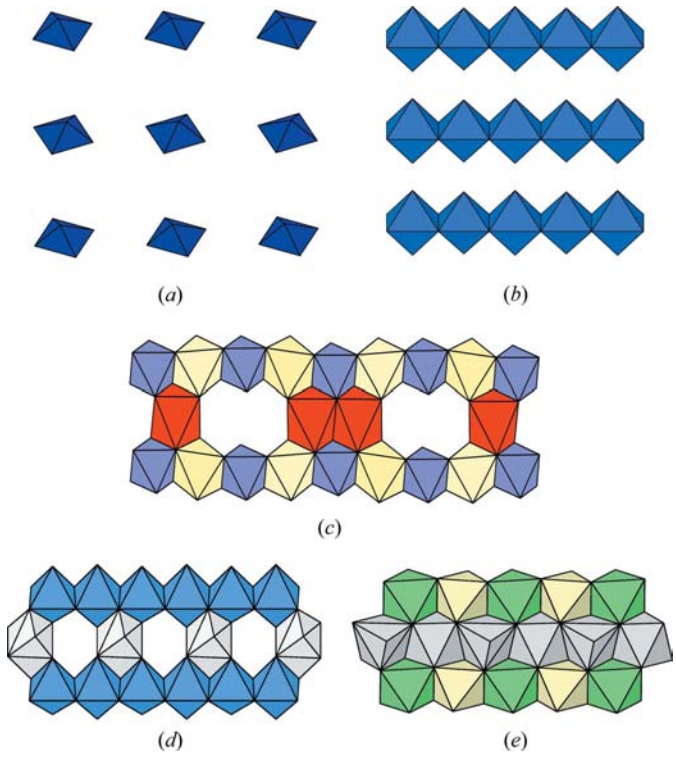

Figure 2
Topologically different *O* sheets in rhodesite-like compounds. (*a*) Seidite-(Ce); (*b*) rhodesite; (*c*) monteregianite; (*d*) TR03; (*e*) TR04.

series. According to the definitions given by Makovicky (1997), the rhodesite series is merotypic because the same silicate module alternates with a variable O module and is plesiotypic because the ratio between the numbers of tetrahedra in the apophyllite-like sheets pointing out and down may vary. The rhodesite-like microporous structure shows at the same time layered and heteropolyhedral-framework features.

Interest in the investigation of the rhodesite-like structures is increasing (*cf.* references given in Table 1) because of their peculiar crystal-chemical, mineralogical and technological aspects. Concerning technology, Rocha *et al.* (1998) have shown that dehydrated synthetic monteregianite (AV-1) and rhodesite (AV-2) can rehydrate; the same two compounds have been used as catalysts for the isomerization of D-glucose to D-fructose (Lima *et al.*, 2008); synthetic rhodesite uptakes ammonia exchanging Na and K (Grutzeck & Marks, 1999); a rhodesite-like phase likely occurs as a product of alkali–silica reaction in concrete (Deceukelaire, 1991).

Extending recent results of our research program (Cadoni & Ferraris, 2009), in this paper we present the synthesis and structural characterization of two new members of the rhodesite series together with a general analysis of the crystal-chemical features of the series.

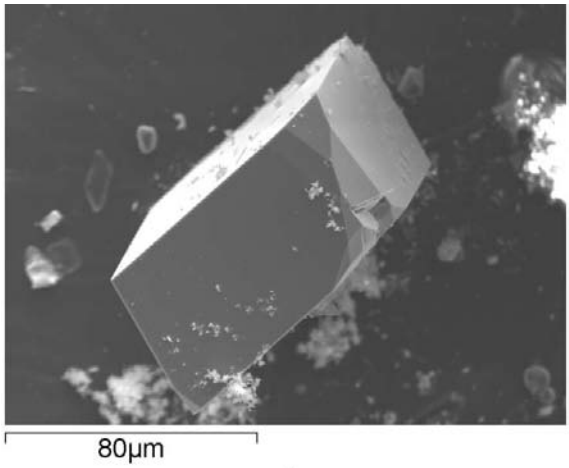

Figure 3
SEM images of (*a*) TR09 and (*b*) TR10.

2. Experimental

2.1. Synthesis

Crystals of $Sr_2Na_2[Si_8O_{19}]\cdot 4H_2O$ (TR09, for short) and $SrNa_4[Si_8O_{19}]\cdot 4H_2O$ (TR10) suitable for single-crystal X-ray diffraction were obtained as products of hydrothermal syntheses aimed at preparing microporous Sr silicates using 25 ml Teflon-lined stainless-steel autoclaves.

TR09 with some amorphous material was obtained from a gel of composition $1SiO_2$:$0.6Na_2O$:0.12Sr:$40H_2O$, autoclaved for 10 d at 503 K. TR10 with minor TR09 was obtained from a gel of composition $1SiO_2$:$0.6Na_2O$:0.08Sr:$40H_2O$, autoclaved for 10 d at 503 K. In both cases the gel was prepared from a strong alkaline solution containing NaOH, NaCl and fumed SiO_2 to which an aqueous solution of $SrCl_2$ was added dropwise and thoroughly stirred (99% pure Aldrich chemicals).

Morphological examination (Fig. 3) and semi-quantitative electron-microprobe chemical analyses were carried out on carbon-coated samples by a scanning electron microscope (Stereoscan S360 Cambridge equipped with an Energy 200 Oxford Instruments EDS apparatus; 15 kV accelerating voltage). The subsequent structure determinations led to the chemical compositions given above.

2.2. Diffraction

X-ray single-crystal diffraction data were collected on an Oxford Gemini R Ultra diffractometer equipped with a CCD area detector (50 kV, 40 mA; graphite-monochromated Mo $K\alpha$ radiation). Information on data collection is given in Table 2.[1] The three-dimensional data were integrated and corrected for Lorentz polarization, background effects and absorption using the package *CrysAlis*^{Pro} (Oxford Diffraction, 2007*a*,*b*). The refinement of the cell parameters (Table 2) was based on all measured reflections with $I_o > 20\sigma(I_o)$.

3. Results

3.1. Structure solution and refinement

The crystal structures of TR09 and TR10 were solved by direct methods and refined using *SHELXL*97 (Sheldrick, 2008) and the *WinGX* package (Farrugia, 1999). Information on the refinements is reported in Table 2.

Except for those bonded to the disordered O*W*2 in TR09, possible positions for the H atoms were spotted as very weak peaks on difference electron-density maps, but their positional parameters could not be satisfactorily refined even by constraining O—H and H···H distances. The residual highest peaks and deepest holes are: 0.67 (close to O*W*2*A*) and −0.77

[1] Supplementary data for this paper are available from the IUCr electronic archives (Reference: WH5008). Services for accessing these data are described at the back of the journal.

Table 2
Experimental details.

For all structures: $Z = 4$. Experiments were carried out at 293 K with Mo $K\alpha$ radiation using an Oxford 'X Calibur Gemini Ultra diffractometer.

	TR09	TR010
Crystal data		
Chemical formula	$Na_2Sr_2Si_8O_{19}\cdot 4H_2O$	$Na_4SrSi_8O_{19}\cdot 4H_2O$
M_r	822.00	780.36
Crystal system, space group	Monoclinic, $C2/c$	Monoclinic, $P2/c$
a, b, c (Å)	22.7681 (2), 6.9352 (1), 13.5789 (1)	22.4102 (3), 7.0292 (1), 13.3140 (2)
β (°)	92.578 (1)	92.538 (1)
V (Å^3)	2141.96 (4)	2095.24 (5)
μ (mm^{-1})	5.58	3.23
Crystal size (mm)	0.10 × 0.10 × 0.06	0.23 × 0.14 × 0.04
Data collection		
Absorption correction	Multi-scan	Multi-scan
T_{min}, T_{max}	0.678, 1.000	0.448, 1.000
No. of measured, independent and observed reflections	33 115, 3801, 3317	27 441, 7247, 5007
Criterion for observed reflections	$I > 2\sigma(I)$	$I > 2\sigma(I)$
R_{int}	0.030	0.034
Refinement		
Refinement on	F^2	F^2
$R[F^2 > 2\sigma(F^2)]$, $wR(F^2)$, S	0.021, 0.080, 0.64	0.033, 0.065, 1.62
No. of reflections	3801	7247
No. of parameters	176	327
No. of restraints	0	2
$\Delta\rho_{max}$, $\Delta\rho_{min}$ (e Å^{-3})	0.67, −0.77	0.83, −0.93

Computer programs: *CrysAlis CCD* (Oxford Diffraction, 2007*a*), *CrysAlis RED* (Oxford Diffraction, 2007*b*), *SHELXS*86 and *SHELXL*97 (Sheldrick, 2008), *ORTEP*3 for Windows (Farrugia, 1997), *ATOMS*6.2 (Dowty, 2002), *WinGX* publication routines (Farrugia, 1999).

(close to Sr) in TR09; 0.83 and −0.93 (both close to O*W*4) in TR10. Both structures have been anisotropically refined except the smaller portion (Na1*B*) of the split Na1 cation in TR09.

4. Structural aspects

Figs. 4, 5 and 6 show the structural features of TR09 and TR10. Tables 3 and 4 report important bond lengths in the two structures.

4.1. H_2O molecules

The O atoms assigned to the H_2O molecules (O*W* in the tables) correspond only to those that do not form Si—O bonds and consequently are strongly underbonded. The possible acceptors of hydrogen bonds have been tested against the expected configuration of H_2O molecules (Chiari & Ferraris, 1982) and the bond valence received from cation–oxygen bonds. The following O*W*···O contacts should correspond to hydrogen bonds. In TR09: O*W*1 with O9 (3.083 Å) and O2 (3.096 Å), O*W*2*A* with O8 (3.12 Å) and O1 (3.24 Å); in TR10: O*W*1 with O12 (2.820 Å) and O*W*3 (2.990 Å), O*W*2 with O5 (2.953 Å) and O*W*4 (3.113 Å), O*W*3 with O3 (2.989 Å) and O14 (3.043 Å), O*W*4 only with O*W*3 (3.188 Å). Based on the given O*W*···O distances, a parameter that is usually used to establish the strength of a hydrogen bond (Chiari & Ferraris, 1982; Ferraris & Ivaldi, 1988), it is clear that most of the H_2O molecules donate only (very) weak hydrogen bonds with the corresponding O···O contacts longer than 3 Å.

The disorder of the O*W*2 oxygen (O*W*2*A*—O*W*2*B* = 0.585 Å) in TR09 is related to that of the Na1 cation (Na1*A*—Na1*B* = 0.365 Å); this rattles around in the large cavity of the *O* sheet which is shaped by the dominating role of the large Sr^{2+} cation, *via* its edge-sharing rows of polyhedra. Even if they are not reported as split, a trend to disorder for H_2O molecules located in channels is revealed by their large displacements factors along [100], *i.e.* across the channels (see §4.2), both in TR09 (O*W*1) and TR10 (O*W*3 and O*W*4). The H_2O molecules not yet mentioned for TR10 (O*W*1 and O*W*2) lie in the *O* sheets.

4.2. The heteropolyhedral framework

Contrary to TR09 and other compounds shown in Table 1, TR10 is based on two crystallographically independent (100) complex modules, each formed by one *O* sheet and two halves of silicate double layers. With reference to cations only, from the top (Fig. 5) one moiety of TR10 contains: Sr1, Na1 and Na2 in the *O* sheet; Si1, Si4, Si6 and Si8 in the silicate part; the second moiety contains: Sr2, Na2 and Na3 in the *O* sheet; Si2, Si3, Si5 and Si7 in the silicate part. Actually, as discussed below, the crystal-chemical differences between the two moieties are small and limited to minor differences in the coordination polyhedra of Sr and one Na; thus only one *O* sheet is shown in Fig. 5(*b*).

In the two structures Na resides both in the *O* sheets (Na2 in TR09; Na1, Na2, Na3 and Na4 in TR10) and at the intersection of the two types of channels that cross the silicate double layer (Na1 in TR09 and Na5 in Tr10). Among the seven-coordinated polyhedra of Na, it is worth noting that in TR10 Na1 lies actually in a 5 + 2 environment with a substantial gap between the fifth (Na1—O*W*1 = 2.634 Å) and the sixth (Na1—O*W*1′ = 2.901 Å) distance. In TR09 Sr shows clearly an eightfold coordination, even if a gap occurs between the longest Sr—O distance (2.782 Å) and the shortest Sr—O*W* split distance (2.95 Å). For the two crystallographically independent Sr cations of TR10 the extension of their coordination sphere beyond six to two next-neighbour O atoms at 3.135 Å (Sr1) and 3.410 Å (Sr2) is weaker but not negligible,

particularly for Sr1. Finally, the degree of octahedral occupancy in the *O* sheets of TR09 (Fig. 4*b*) and TR10 (Fig. 6*b*) is different and corresponds to that of topologies shown in Figs. 2(*d*) and (*e*), respectively.

Among the known compounds with rhodesite-like structure (Table 1), TR09 and TR10 are the only ones where the cross sections of both systems of eight-membered channels are strongly anisotropic (Figs. 4, 5 and 6). In TR10 the e.c.w. value of both independent channels that develop perpendicularly to the octahedral rows, *i.e.* along [001], is *ca* 2.7 × 4.3 Å; the corresponding value for the two independent channels running along [010] is *ca* 1.2 × 5.2 Å. In TR09 the e.c.w. values are 2.5 × 4.2 and 2.2 × 4.3 Å along [001] and [010]. The large Sr cation is the source of stress leading to the squeezing of all channels.

4.3. Crystal-chemical features of the rhodesite series

As explained in §1 the known compounds with a rhodesite-like structure (Table 1) belong to a mero-plesiotype series built by alternating 'octahedral' and tetrahedral modules that, while preserving a layered character, are connected to form a microporous heteropolyhedral framework (Figs. 1, 4 and 5). The increasing number of known members (seven minerals and ten synthetic phases) reflects a versatility of the structural edifice that is allowed by the following crystal-chemical features, mainly related to the heteropolyhedral nature of the framework.

(i) Based on the degree of cation deficiency, five different *O* modules have been found (Fig. 2): isolated octahedra, isolated rows of edge-sharing octahedra, alternation between continuous and fragmented rows of octahedra, full sheet of octahedra.

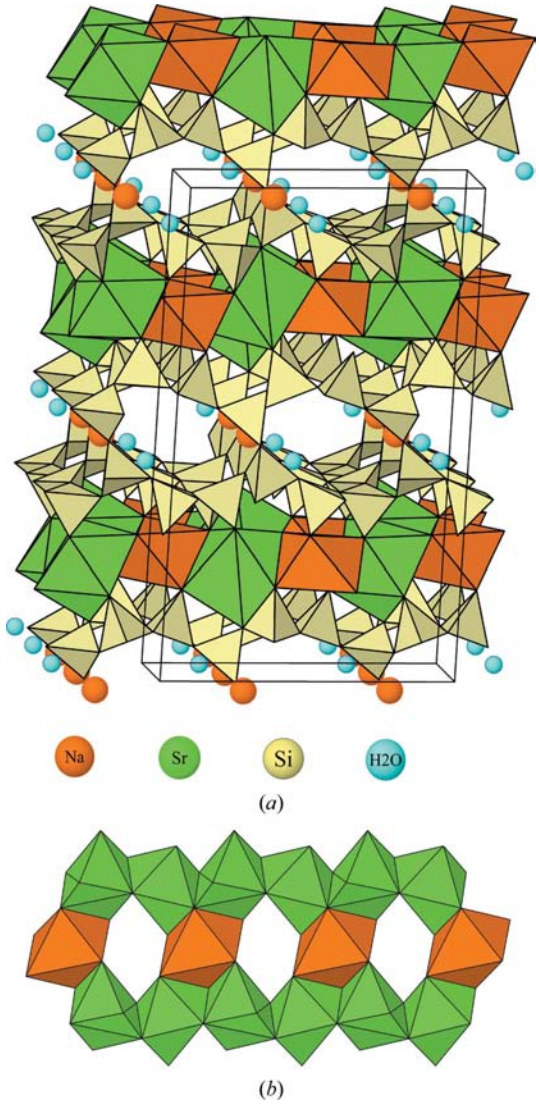

Figure 4
Crystal structure of TR09 seen approximately along (*a*) [010] (*x* axis vertical) and (*b*) the corresponding *O* sheet.

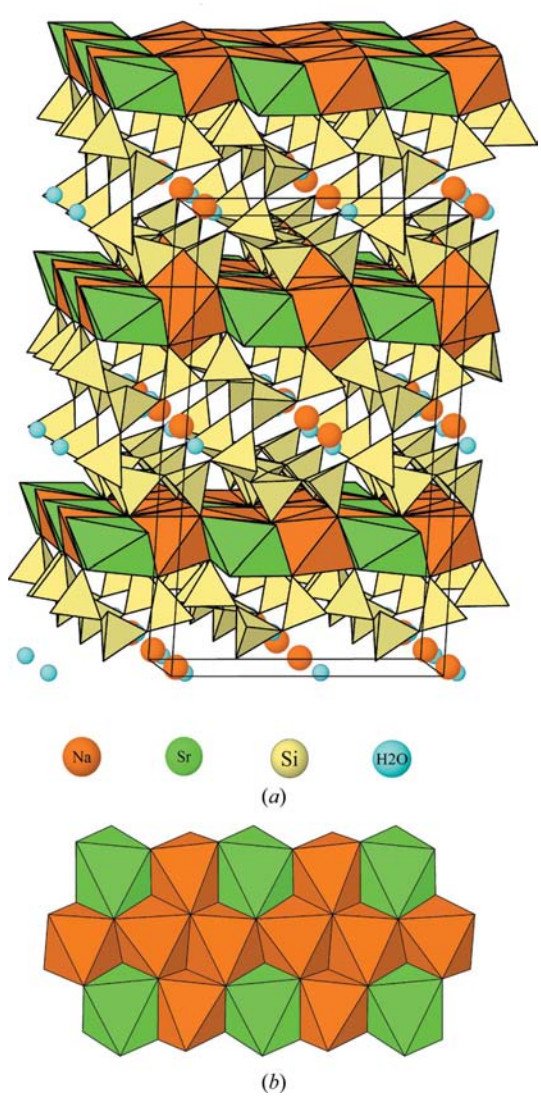

Figure 5
Crystal structure of TR10 seen approximately along (*a*) [010] (*x* axis vertical) and (*b*) the corresponding *O* sheet. For an easier comparison with TR09 the origin is shifted about 1/4 along the *x* axis.

Table 3
Important bond distances (Å) for TR09; O*W* represents the O atoms of the H_2O molecules.

Sr—O10	2.458 (1)	Si1—O1	1.572 (1)
Sr—O8	2.465 (2)	Si1—O2	1.626 (1)
Sr—O1	2.488 (1)	Si1—O3	1.637 (1)
Sr—O1	2.518 (1)	Si1—O4	1.653 (1)
Sr—O10	2.591 (1)		
Sr—O6	2.782 (1)	Si2—O5	1.597 (1)
Sr—O*W*2*B*	2.95 (1)	Si2—O6	1.609 (1)
Sr—O*W*2*B*	2.96 (1)	Si2—O4	1.618 (1)
Sr—O*W*2*A*	2.99 (1)	Si2—O7	1.626 (1)
Sr—O*W*2*A*	3.08 (1)		
		Si3—O8	1.571 (2)
Na1*A*—O8	2.299 (6)	Si3—O2	1.633 (1)
Na1*A*—O*W*2*B*	2.38 (3)	Si3—O5	1.633 (1)
Na1*A*—O10	2.404 (6)	Si3—O9	1.638 (1)
Na1*A*—O10	2.413 (6)		
Na1*A*—O*W*2*A*	2.50 (3)	Si4—O10	1.573 (1)
Na1*A*—O8	2.52 (2)	Si4—O9	1.622 (1)
		Si4—O3	1.627 (1)
Na1*B*—O10 × 2	2.381 (1)	Si4—O6	1.653 (1)
Na1*B*—O8 × 2	2.381 (1)		
Na1*B*—O*W*2*B* × 2	2.73 (1)		
Na1*B*—O*W*2*A* × 2	2.855 (8)		
Na2—O*W*1 × 2	2.382 (2)		
Na2—O4 × 2	2.573 (2)		
Na2—O3 × 2	2.648 (1)		
Na2—O7	2.741 (2)		

(ii) If the occurrence of rows with mixed cations, coordination numbers other than six, cations with different charges and a variety of anions (or H_2O) were taken into account, the number of different *O* sheets would dramatically increase.

(iii) The charge of the typical silicate double layer $[Si_8O_{19}]^{-6}$ can be modified by Al → Si and OH → O substitutions. If the content of the channels is included, the charge flexibility of the microporous layer can further increase because both cations and anions (*e.g.* Cl in delhayelite and fivegite) can be located there.

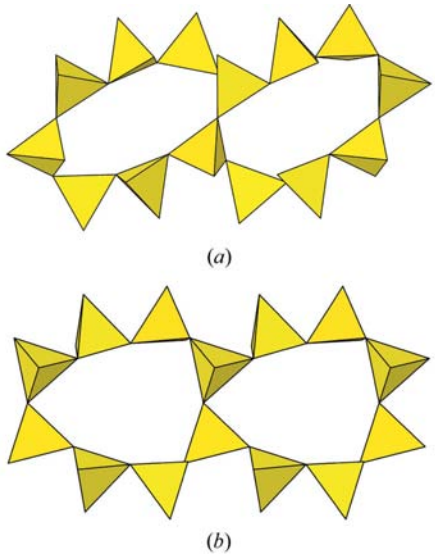

Figure 6
Highly distorted channels delimited by eight-rings that occur in the double silicate layer of TR09 and TR10 as seen along (*a*) [010] and (*b*) [001].

Table 4
Important bond distances (Å) for TR10.

Sr1—O17 ×2	2.500 (2)	Si1—O1	1.605 (2)
Sr1—O12 ×2	2.511 (2)	Si1—O2	1.605 (2)
Sr1—O19 ×2	2.696 (2)	Si1—O3	1.610 (2)
		Si1—O4	1.612 (2)
Sr2—O15 ×2	2.459 (2)		
Sr2—O9 ×2	2.520 (2)	Si2—O5	1.574 (2)
Sr2—O5 ×2	2.663 (2)	Si2—O6	1.635 (2)
		Si2—O7	1.636 (2)
Na1—O12	2.330 (2)	Si2—O8	1.652 (2)
Na1—O17	2.344 (2)		
Na1—O19	2.414 (2)	Si3—O9	1.576 (2)
Na1—O19	2.513 (2)	Si3—O10	1.622 (2)
Na1—O*W*1	2.658 (3)	Si3—O11	1.641 (2)
Na1—O*W*1	2.897 (3)	Si3—O7	1.648 (2)
Na1—O14	3.062 (2)		
		Si4—O12	1.578 (2)
Na2—O17 ×2	2.334 (2)	Si4—O13	1.619 (2)
Na2—O12 ×2	2.410 (2)	Si4—O1	1.632 (2)
Na2—O*W*1 ×2	2.539 (3)	Si4—O14	1.639 (2)
Na3—O9	2.261 (2)	Si5—O15	1.574 (2)
Na3—O15	2.428 (2)	Si5—O10	1.623 (2)
Na3—O5	2.498 (2)	Si5—O16	1.630 (2)
Na3—O5	2.564 (2)	Si5—O6	1.649 (2)
Na3—O*W*2	2.705 (4)		
Na3—O6	2.852 (2)	Si6—O17	1.577 (2)
Na3—O*W*2	2.883 (3)	Si6—O13	1.625 (2)
		Si6—O18	1.638 (2)
Na4—O9 ×2	2.407 (2)	Si6—O3	1.645 (2)
Na4—O15 ×2	2.410 (2)		
Na4—O*W*2 ×2	2.507 (2)	Si7—O16	1.602 (2)
		Si7—O2	1.606 (2)
Na5—O*W*4	2.339 (3)	Si7—O11	1.609 (2)
Na5—O*W*3	2.380 (3)	Si7—O8	1.618 (2)
Na5—O7	2.523 (2)		
Na5—O18	2.544 (2)	Si8—O19	1.574 (2)
Na5—O4	2.564 (2)	Si8—O18	1.633 (2)
Na5—O8	2.601 (2)	Si8—O14	1.637 (2)
		Si8—O4	1.652 (2)

(iv) The same cation can lie both in the *O* sheet and in the channels of the silicate layer.

(v) Most of the hydrogen bonds involving the H_2O molecules, particularly those located in the channels, are (very) weak; that favours splitting and/or apparent very anisotropic displacement factors of the corresponding O atoms. This type of H_2O molecule can display a zeolitic behaviour as Rocha *et al.* (1998) have shown by dehydrating and rehydrating synthetic monteregianite (AV-1) and rhodesite (AV-2).

In spite of the wide compositional range that occurs in the series, the overall conformation of the silicate double layer tends to stay constant and the two systems of intersecting channels tend to maintain cross sections close to those reported above for rhodesite. Only the presence of Sr^{2+} in the *O* sheet has a strong influence on the configuration of the double layer. In fact, because of the larger ionic radius and the consequent larger coordination sphere of this cation, in TR09 and TR10 all channels are squeezed and assume a lance-top shape (Fig. 6).

As already noted by Ferraris & Gula (2005), a microporous silicate double layer similar to that of rhodesite occurs in the structure types represented by reyerite $[Ca_{14}(Na,K)_2Si_{22}Al_2O_{58}(OH)_8{\cdot}6H_2O$; a = 9.765, c = 19.067 Å, $P\bar{3}$; Merlino, 1988*a*] and fedorite $[K_2(Ca_5Na_2)Si_{16}O_{38}(OH,F)_2{\cdot}H_2O$; $a = b$ =

9.67, c = 12.67 Å, α = 102.2, β = 71.2, γ = 120.0°, $P\bar{1}$; Merlino, 1988*b*]. However, in both these minerals the apophyllite-like silicate sheet with topology $4^1 8^1$ is replaced by a silicate sheet containing only six-rings.

5. Conclusions

The synthesis and subsequent structural characterization of two new members of the rhodesite mero-plesiotype series and the recent description of a new mineral belonging to the same series (Pekov *et al.*, 2010) further prove the versatility of the microporous rhodesite-type heteropolyhedral framework, as discussed in this article in terms of crystal-chemical features. In particular, the possibility of introducing lanthanides in the *O* sheet (Table 1) attracts the attention of materials scientists. In fact, the luminescent properties of a lanthanide can be modulated playing on the variety of structural environments that can host this cation, thanks to the flexibility of the heteropolyhedral framework, in particular of the *O* sheet (Fig. 1). Finally, we have discussed the influence that a large cation, namely Sr^{2+}, occurring in the *O* sheet has on the e.c.w. of the channels and, consequently, on the porosity and exchange possibilities of the heteropolyhedral framework.

This work was financially supported by MIUR [Roma, project PRIN 2007 'Compositional and structural complexity in minerals (crystal chemistry, microstructures, modularity, modulations): analysis and applications']. We are grateful to Igor V. Pekov (Moscow University) for communicating unpublished results on minerals of the rhodesite series. The constructive comments of two anonymous reviewers and of the co-editor helped to improve the text.

References

Ananias, D., Ferreira, A., Rocha, J., Ferreira, P., Rainho, J. P., Morais, C. & Carlos, L. D. (2001). *J. Am. Chem. Soc.* **123**, 5735–5742.
Ananias, D., Rainho, J. P., Ferreira, A., Rocha, J. & Carlos, L. D. (2004). *J. Alloys Compd.* **374**, 219–222.
Cadoni, M. & Ferraris, G. (2009). *Eur. J. Mineral.* **21**, 485–493.
Cannillo, E., Rossi, G., Ungaretti, L. & Carobbi, S. G. (1968). *Atti Accad. Naz. Lincei Classe Sci. Fis.* **45**, 399–414.
Chiari, G. & Ferraris, G. (1982). *Acta Cryst.* B**38**, 2331–2341.
Chiragov, M. I. & Dorfman, M. D. (1981). *Dokl. Akad. Nauk SSSR*, **260**, 458–461 (in Russian).
Deceukelaire, L. (1991). *Mater. Struct.* **24**, 169–171.
Dorfman, M. D. & Chiragov, M. I. (1979). *New Data Miner. USSR*, **28**, 172–175 (in Russian).
Dowty, E. (2002). *ATOMS*, Version 6.2. Shape Software, 521 Hidden Valley Road, Kingsport, Tennessee, USA.
Farrugia, L. J. (1997). *J. Appl. Cryst.* **30**, 565.
Farrugia, L. J. (1999). *J. Appl. Cryst.* **32**, 837–838.
Ferraris, G., Belluso, E., Gula, A., Khomyakov, A. P. & Soboleva, S. V. (2003). *Can. Mineral.* **41**, 1183–1192.
Ferraris, G. & Gula, A. (2005). *Rev. Mineral. Geochem.* **57**, 69–104.
Ferraris, G. & Ivaldi, G. (1988). *Acta Cryst.* B**44**, 341–344.
Ferraris, G., Makovicky, E. & Merlino, S. (2008). *Crystallography of Modular Materials.* Oxford University Press.
Ferraris, G. & Merlino, S. (2005). Editors. *Micro- and Mesoporous Mineral Phases.* Washington DC: Mineralogical Society of America, Geochemical Society.
Ghose, S., Sen Gupta, P. K. & Campana, C. F. (1987). *Am. Mineral.* **72**, 365–374.
Grutzeck, M. W. & Marks, J. A. (1999). *Environ. Sci. Technol.* **33**, 312–317.
Hesse, K. F., Liebau, F. & Merlino, S. (1992). *Z. Kristallogr.* **199**, 25–48.
Krivovichev, S. V. (2009). *Structural Crystallography of Inorganic Oxysalts.* Oxford University Press.
Lima, S., Dias, A. S., Lin, Z., Brandão, P., Ferreira, P., Pillinger, M., Rocha, J., Calvino-Casilda, V. & Valente, A. A. (2008). *Appl. Catal. Gen.* **339**, 21–27.
Makovicky, E. (1997). *EMU Notes Mineral.* **1**, 315–344.
McCusker, L. B., Liebau, F. & Engelhardt, G. (2003). *Micropor. Mesopor. Mater.* **58**, 3–13.
Merlino, S. (1988*a*). *Mineral. Mag.* **52**, 247–256.
Merlino, S. (1988*b*). *Mineral. Mag.* **52**, 377–387.
Oxford Diffraction (2007*a*). *CrysAlis CCD*. Oxford Diffraction Ltd, Abingdon, Oxfordshire, England.
Oxford Diffraction (2007*b*). *CrysAlis RED*. Oxford Diffraction Ltd, Abingdon, Oxfordshire, England.
Pekov, I. V., Zubkova, N. V., Chukanov, N. V., Sharygin, V. V. & Pushcharovskii, D. Yu. (2009). *Dokl. Earth Sci.* **428**, 1216–1221.
Pekov, I. V., Zubkova, N. V., Chukanov, N. V., Zadov, A. E. & Pushcharovskii, D. Yu. (2010). *Zapiski RMO.* In the press.
Ragimov, K. G., Chiragov, M. I., Mamedov, K. S. & Dorfman, M. D. (1980). *Dokl. Akad. Nauk Aze. SSR*, **36**, 49–51 (in Russian).
Rocha, J., Carlos, L. D., Ferreira, A., Rainho, J., Ananias, D. & Lin, Z. (2004). *Mater. Sci. Forum*, **455–456**, 527–531.
Rocha, J., Ferreira, P., Carlos, L. D. & Ferreira, A. (2000). *Angew. Chem. Int. Ed.* **39**, 3276–3279.
Rocha, J., Ferreira, P., Lin, Z., Brandão, P., Ferreira, A. & Pedrosa de Jesus, J. D. (1998). *J. Phys. Chem. B*, **102**, 4739–4744.
Rocha, J. & Lin, Z. (2005). *Rev. Mineral. Geochem.* **57**, 173–201.
Sheldrick, G. M. (2008). *Acta Cryst.* A**64**, 112–122.